J. Cosmet. Sci., **67,** 21–36 (January/February 2016)

Harvesting electricity from human hair

BRINDAN TULACHAN, SUSHIL K. SINGH, DEEPU PHILIP, and MAINAK DAS, *Biological Sciences & Bioengineering, Indian Institute of Technology Kanpur, Kanpur 208016, UP, India (B.T.); Solid State Physics Laboratory, DRD0, Delhi 110054, India (S.K.S.); Industrial & Management Engineering, Indian Institute of Technology Kanpur, Kanpur 208016, UP, India (D.P.); and Design Program, Indian Institute of Technology Kanpur, Kanpur 208016, UP, India (D.P., M.D.).*

Accepted for publication November 3, 2105.

Synopsis

Electrical conductivity of human hair is a debatable issue among hair experts and scientists. There are unsubstantiated claims that hair conducts electricity. However, hair experts provided ample evidence that hair is an insulator. Although wet hair exhibited drastic reduction in resistivity; scientists regarded hair as a proton semiconductor at the best. Here, we demonstrate that hair filaments generate electricity on absorbing water vapor between 50° and 80°C. This electricity can operate low power electronic systems. Essentially, we are exposing the hydrated hair polymer to a high temperature (50°–80°C). It has long been speculated that when certain biopolymers are simultaneously hydrated and exposed to high temperature, they exhibit significant proton hopping at a specific temperature regime. This happens due to rapid movement of water molecules on the polymer surface. This lead us to speculate that the observed flow of current is partly ionic and partly due to "proton hopping" in the hydrated nano spaces of hair filament. Such proton hopping is exceptionally high when the hydrated hair polymer is exposed to a temperature between 50° and 80°C. Differential scanning calorimetry data further corroborated the results and indicated that indeed at this temperature range, there is an enormous movement of water molecules on the hair polymer surface. This enormously rapid movement of water molecules lead to the "making and breaking" of innumerable hydrogen bonds and thus resulting in hopping of the protons. What is challenging is "how to tap these hopping protons to obtain useful electricity?" We achieved this by placing a bundle of hair between two different electrodes having different electro negativities, and exposing it to water vapor (water + heat). The two different electrodes offered directionality to the hopping protons and the existing ions and thus resulting in the generation of useful current. Further, by continuously hydrating the polymer with water vapor, we prolonged the process. If this interesting aspect of polymer is exploited further and fine tuned, then it will open new avenues for development of sophisticated polymer-based systems, which could be used to harvest electricity from waste heat.

INTRODUCTION

Human hair is a hot topic of debate on its electrical conductivity properties (1–5). To better understand the electrical properties of hair, the architecture of human hair is to be carefully examined (6–8). Human hair is a self-assembly of concentric, cylindrical, and structural composites; with each concentric cylinder having different compositions and associated functional properties. It resembles monofilaments under microscope,

Address all correspondence to Mainak Das at mainakd@iitk.ac.in

with roof tiles like overlapping scales, till the tip of the fiber. The outermost concentric cylinder called cuticle consists of plate-shaped cells, scales, which overlap both longitudinally and peripherally. Cuticle is mainly composed of structural and free lipids surrounding the dead cells with inner volume of the cells filled with keratin protein. The middle layer is the bulk of the volume consisting of spindle-shaped dead cells filled with α-keratin and keratin-associated proteins. However, the innermost cylindrical yet discontinuous layer consists of cells filled with melanin pigments, which is known for its semiconductor properties (9–12) and ultraviolet absorption capabilities (Figure 1 A, B).

The overall architecture of the hair resembles a GAU-8 Avenger gun barrel of late Nineteen seventies (1970s) in nanoscale, where the metallic barrel is replaced with "protein nanotubes". Each spindle-shaped dead cell in cortex consists of five to eight macrofibrils. Individual macrofibril comprises of 500–800 microfibrils, where each microfibril is made up of seven to eight protofilaments. Each protofilament is a self-assembly of four chain structures called tetramer of α-keratin and keratin-associated proteins (Figure 1 C). α-Keratin protein is the major component of human hair (including wool), horns, nails, hooves, and claws of mammals (5,7,8).

Eminent hair experts have provided ample proof that α-keratin protein in hair is an insulator (4,5,13–15) It has been demonstrated that resistivity value of hair changes with water content. The wool–water system with 7% water content, exhibited a resistivity of 3×10^{12} ohm cm at room temperature; whereas, at 25% of water content, the resistivity decreased to 6×10^{6} ohm cm at room temperature. It has been concluded that even at high moisture content, α-keratin is a poor conductor of electricity (4,5,13–20).

The scientists considered hair as a proton semiconductor to explain the limited electrical conductivity of a keratin–water system, which is the same as that of ice, nylon–water, and cellulose–water system (4,5,14,21–26). This conduction mechanism depends on a continuous hydrogen bond network that is formed between the water and keratin molecules. This network facilitates conduction by proton hopping, which explains why wet hair exhibited lower resistivity.

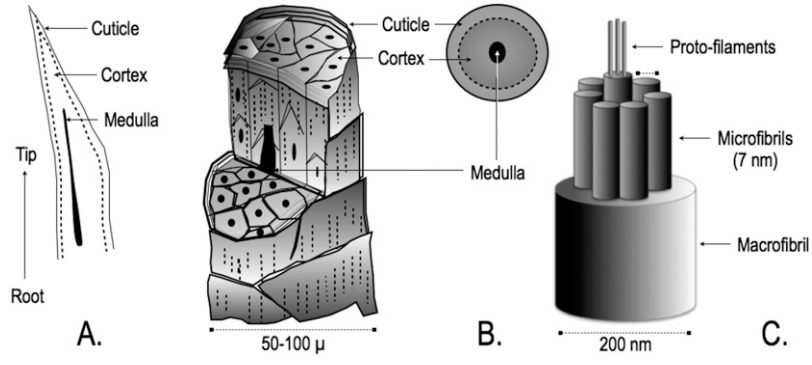

Figure 1. Anatomy of hair. (A) Longitudinal section of a single hair fiber. (B) Longitudinal section of the hair showing the detailed cellular architecture. Transverse cross-section showing the large cortical region. (C) Arrangement of α-keratin protein inside the cortical cells.

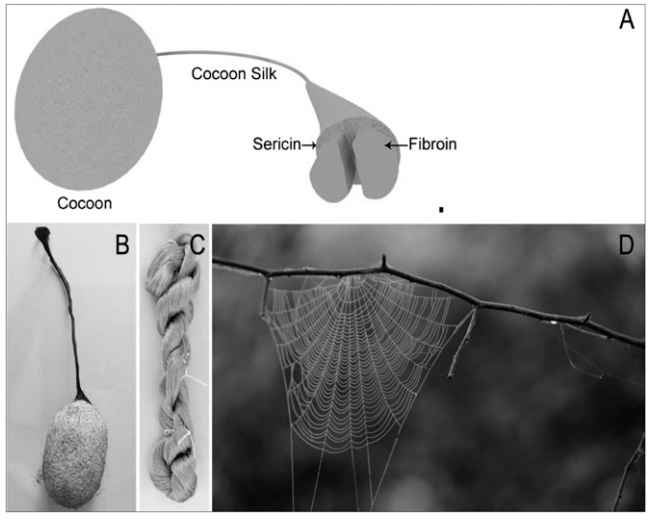

Figure 2. World of silk. (A) Schematic diagram showing the overall molecular architecture of silk cocoon and unprocessed silk thread. The silk cocoon is made up of these individual silk fibers. Individual silk fibers consists of two proteins viz. an outer gummy protein called sericin and an inner core forming the actual silk thread called fibroin. The silk threads adhere to each other by sticky sericin protein thus forming the rigid architecture of the silk cocoon. (B) *A. mylitta* silk cocoon, a wild non-mulberry silk. (C) Processed non-mulberry silk thread after degumming, which is used for textile. (D) Spider silk lacking gummy sericin protein and that is the reason why the individual threads could be observed.

In this report, we studied the electrical conductivity of dry hair, wet hair, and hair exposed to water vapor (water + heat) and performed a comparative study with two other natural fibrous proteins viz. mulberry (*Bombyx mori*) and non-mulberry *Antheraea mylitta*) silk (Figure 2)(26). Further using human hair, we developed a simple bio-electric device, which on exposure to water vapor generates sufficient electricity so as to operate low power electronic systems. We have further performed a comparative differential scanning calorimetric (DSC) study of hair and silk fiber in dry and hydrated conditions

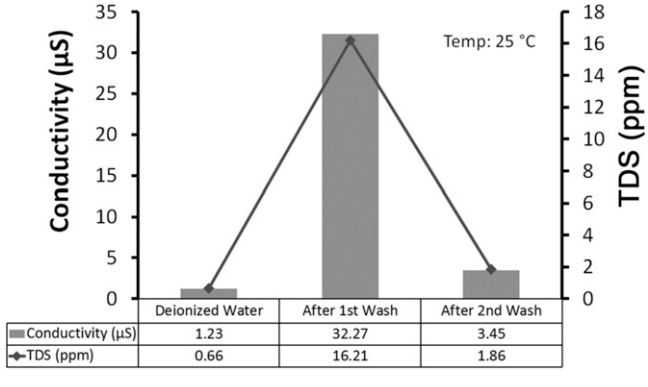

Figure 3. Conductivity and total dissolved solute (TDS) of the pure deionized water, deionized water after first hair wash and deionized water after second hair wash. The hair was used after second wash for the experiment. A bath ratio of 5:1 of human hair in mg and deionized water in ml was used in each soak. Cyberscan Con 11; Eutech instruments was used at room temperature 25 °C for measuring the conductivity and TDS.

Table I
Hair and Silk Cocoon Membrane

	Configuration I	Configuration II	Configuration III
Electrode 1 (E1)	Copper	Platinum	Copper
Electrode 2 (E2)	Copper	Aluminum	Aluminum

and showed that a rapid motion of water molecules takes place at temperature around 80°C, which resulted in generation of large number of protons on the surface of these biopolymers. This partly explains the observed maximum conductivity is observed around 50°–80°C. This finding is important because if such devices could be developed using biopolymers, then these will be useful to harness electrical energy from waste heat contained in the exhaust steam of thermal and nuclear power plants, as well as

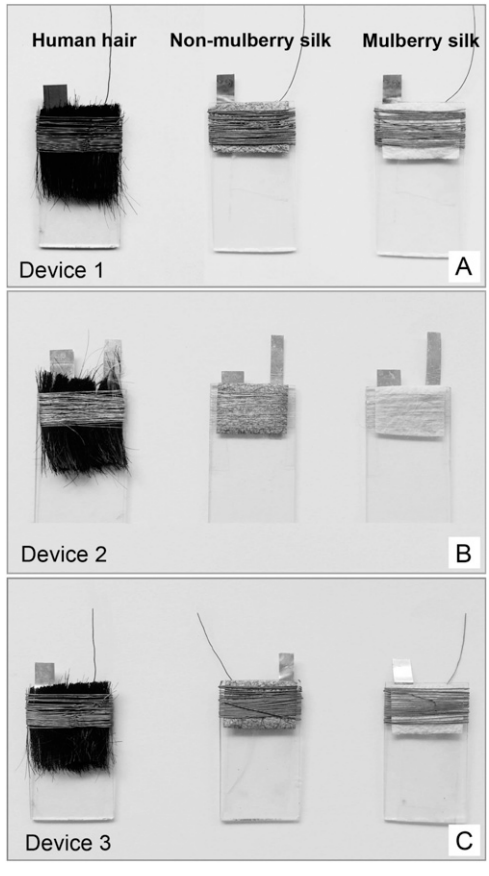

Figure 4. Standard device fabricated by connecting the two similar and dissimilar electrodes to study the electrical properties of human hair and silk cocoon membrane. This uniform device helps in comparing the data obtained from different sources. (A) Two copper electrodes attached with colloidal silver paste for making proper connections. The first device is prepared with human hair. Second and third devices were prepared with *A. mylitta* silk cocoon with average natural thickness 0.5 mm and *B. mori* silk cocoon membrane with an average thickness of 0.5 mm. (B) Simple device was made by connecting the two different electrodes on the surface composed of aluminum and platinum. (C) Device prepared with aluminum and copper electrodes.

from the buildings in the winter, where a large amount of heat energy is needed to maintain the temperature.

MATERIALS AND METHODS

COLLECTION OF HAIR SAMPLES AND PROCESSING

Hairs from random individuals were collected, and washed with deionized water twice for an hour. This wet hair was then allowed to dry in a laminar flow hood at room temperature. One of challenging problem is to wash the hair sample and to ensure the removal of the ionic species (27). Thus we conducted a simple test to ensure that most of the loosely bound ionic species are removed during washing. We first measured the conductivity of the deionized water to be used for washing the hair (Figure 3). Next, we kept the hair sample in this water and used a magnetic stirrer to swirl the water for 30 min, thus ensuring that all the loosely bound ionic species present in water gets dissolved in water. After the first wash, we measured the conductivity of the water. We observed a significant increase in conductivity, thus indicating the presence of ionic species which has leached out from the hair surface. Again we repeated the process for 30 min and measured the conductivity. We observed that the conductivity of water falls down to the baseline. This experiment ensured that the removal of the ionic species and proper washing of the hair.

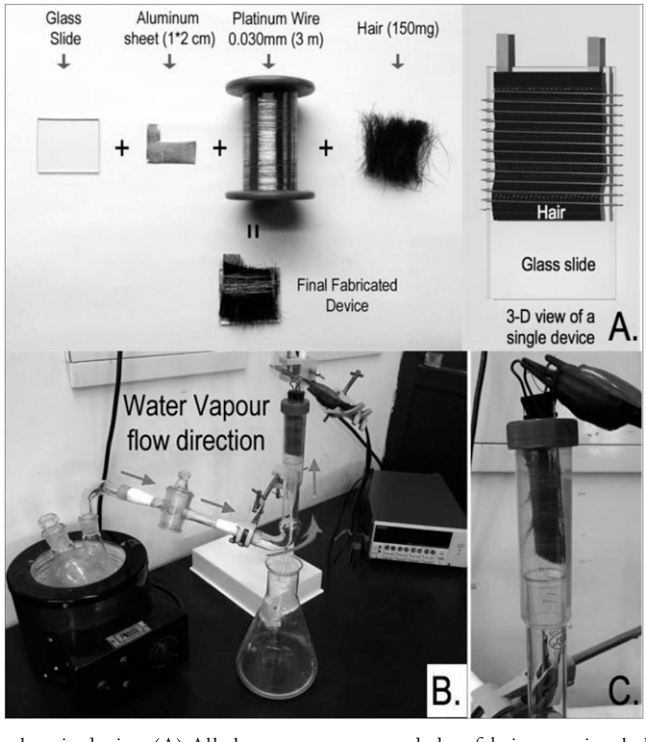

Figure 5. Hair bioelectric device. (A) All the components needed to fabricate a simple hair bioelectric device. (B). The overall test apparatus showing the source of water vapor. (C) The bioelectric device inside the plastic casing attached to the glass tube supplying water vapor.

COLLECTION OF MULBERRY (*B. MORI*) AND NON-MULBERRY (*A. MYLITTA*) SILK COCOONS

The mulberry and non-mulberry silk cocoons were collected from the silk farmers residing in the Indian states of Karnataka and Chattishgarh, respectively. These cocoons were cleaned with a dry blower and stored in a desiccator (26).

SCANNING ELECTRON MICROSCOPY

The morphology of the hair and silk cocoon membrane was studied using scanning electron microscopy (SEM; SUPRA 40VP field emission SEM, Carl Zeiss NTS GmbH, Oberkochen, Germany).

SELECTION OF ELECTRODE MATERIALS AND DEVELOPING THE MEASUREMENT SETUP

Aluminum, platinum, and copper were chosen as the electrode metals. A glass slide was used as the holding frame, on which electrode (E1) was fixed. Then, 150 grams of dried human hair was spread evenly covering the electrode (E1). In case of silk, the silk cocoon membrane was fixed on top of E1. The counter electrode (E2) wire was wounded over the whole setup covering the hair/silk cocoon membrane substantially, forming the measurement device; with hair/ silk sandwiched between the electrode

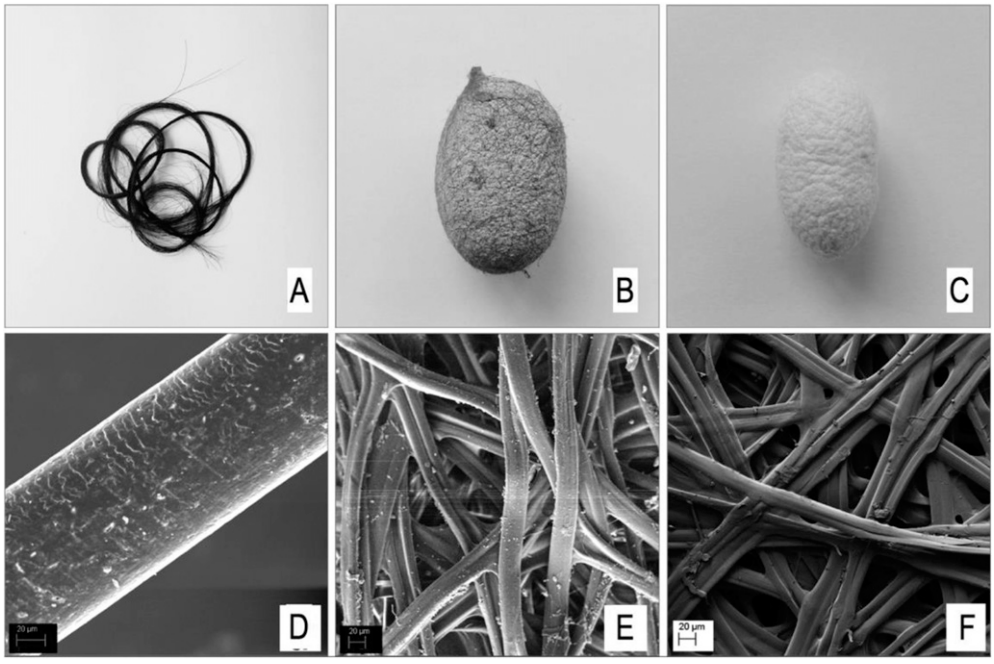

Figure 6. Gross and scanning electron microscopic morphology of Human hair and Silk Cocoon. (A) Natural human hair with black texture. (B, C) *A. mylitta* silk cocoon has brownish coarse texture while *B. mori* cocoon has a soft texture. (D) Scanning Electron Microscopy image of the surface of a human hair showing cuticle (scales) on outside of our hair. (E, F) Rough outer surface of *A. mylitta* with some crystals of calcium oxalates and smooth outer surface of the *B. mori* cocoon.

metals. All voltage and current measurements were made using this "hair/silk measurement device". Three different electrode configurations used in the study are shown in Table 1.

Three different electrode configurations (I–III) were used for recording the current and voltages across hair and silk cocoon membrane. In configuration I, same electrodes were used across the membrane. In configuration II and III, different electrodes were used. For configuration I, high-purity copper wires of 32 AWG (1.2-m long) and 32-gauge copper sheets (1×2 cm^2 area) were used. While for configuration II, high-purity platinum wire of 49 AWG (3-m long) and 32 gauge aluminum sheets (1×2 cm^2 area) were used and for configuration III, high-purity copper wires of 32 AWG (1.2-m long) and 32-gauge aluminum sheets (1×2 cm^2 area) were used as electrodes.

We either use same copper electrode as E1 and E2 (Figure 4A), or dissimilar electrodes (Figure 4B, C). The figure 4A –C is showing some simple devices fabricated by us, using human hair and silk. Three different electrode configurations (E1:E2) were used to perform the recordings.

ELECTRICAL MEASUREMENTS

The current and voltage across the measurement device was recorded using an electrometer Keithley's 51/2-digit Model 6517B electrometer/high resistance meter (Keithley

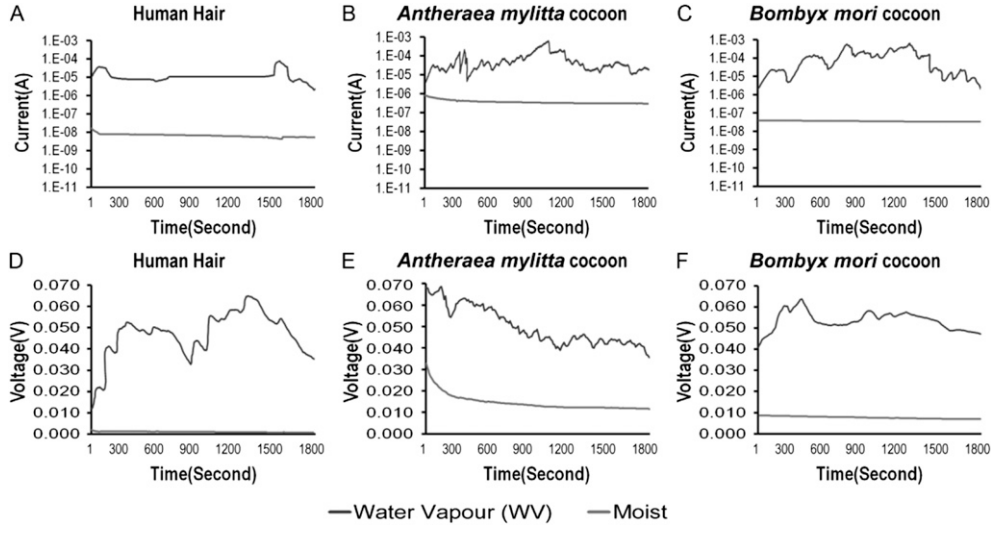

Figure 7. Electrical properties of human hair and silk cocoon sandwiched between same copper electrodes (Device 1). Representative traces of current and voltage obtained from bioelectric device described in Figure 4. (A) Average (n = 6) current profiles of human hair under the two different conditions (moist and exposed to water vapor), in moist state the average current value is around 9.57185E-09 while it increases drastically to 8.65487E-06 when exposed to water vapor. (B, C) Trend is almost identical in the silk cocoon but the average current density is higher as compared to the human hair. When exposed to water vapor average current density in (B) A. mylitta is 7.98428E-05 which is higher than (C) B. mori 6.48795E-05, as it has more ion species inherently present in them. (D) Average voltage recording obtained from human hair shows that there is negligible voltage when moist, while when exposed to water vapor the voltage rises sharply. (E, F) Pattern of average voltage reading of silk cocoon membrane is similar to that observed in human hair. Voltage is low in moist conditions and increases sharply, when exposed to water vapor.

Instruments, Inc., Cleveland, OH). Average trace of current and voltage obtained from 10 such devices of each type of electrode configuration is depicted in the results. The 6517A/B Electrometer/high resistance meter basic application software written on LabVIEW 8.6 was used for the recording of devices which was interfaced with computer. To find the basic average of six replicates, all we had to do is add all the recording and divide the resultant by six and plot the graph in Microsoft Excel 2014. The polarities of the various devices were as follows:

Device 1: copper winding as positive terminal and copper sheet as negative terminal.
Device 2: platinum winding as positive terminal and aluminum sheet as negative terminal.
Device 3: copper winding as positive terminal and aluminum sheet as negative terminal.

HAIR BIOELECTRICAL DEVICE FOR ENERGY HARVESTING

Two different configurations of simple bioelectrical devices were assembled. Here, we are providing the graphics of one such configuration, where a plastic casing covered the device to ensure uniform application of water vapor on human hair. Pure deionized water was boiled to generate water vapor, which was then directed to the plastic casing using bent glass tubes; subjecting the device assembly to external stimulus. When water vapor reached the bioelectric device, its temperature was around 80°–85°C (Figure 5). In the Results section, we have provided another configuration of the same device as described below. It is just fabricated with copper and aluminum and mounted on a glass rod.

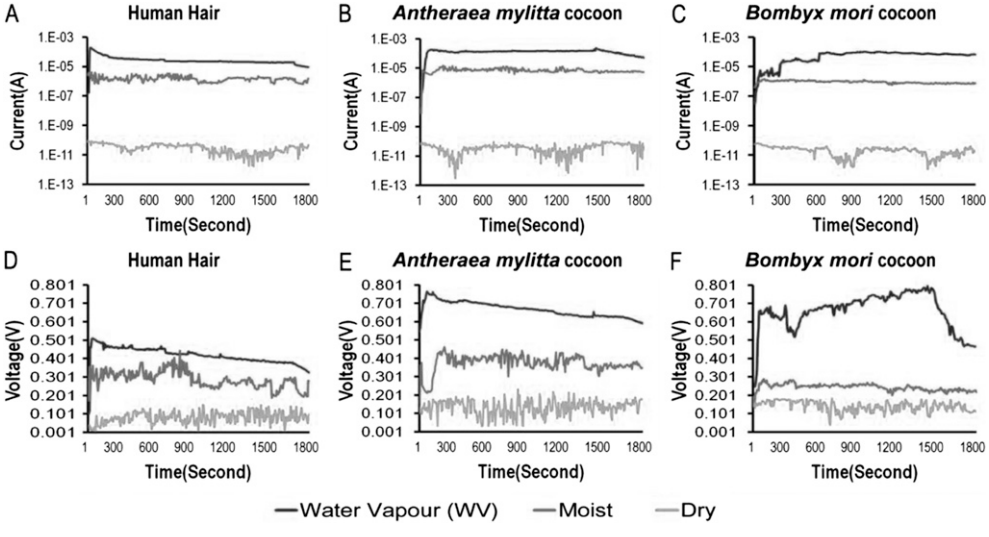

Figure 8. Electrical properties of human hair and silk cocoon sandwiched between aluminum and Copper. Three different conditions were kept dry, moist, and exposed to water vapor. (A) Average (n = 6) current reading for human hair which shows the trend is almost identical to that observed in Figure 7. Behaving as an insulator in dry state and when came in contact with moisture the current values shoot up sharply. (B, C) Average current reading obtained from silk cocoon showing similar pattern as observed in previously published work (26). (D) Average voltage reading obtained from human hair. Here we cannot observe the hump around 1600 s that we observed with aluminum and platinum (Figure 9). Instead the voltage is decreasing sharply once the water vapor was stopped. (E, F) Similar reading could be seen in silk cocoons.

ELECTRICAL RECORDINGS FROM DRY, MOIST, AND WATER VAPOR-EXPOSED HAIR

The electrical recordings were performed in three conditions viz., dry, moist, and water vapor. The dry and water vapor recordings were straight forward. The moist hair is prepared by cooling the hair for 30 min in room temperature after it was exposed to water vapor.

RESULTS

ULTRASTRUCTURE OF HAIR AND SILK COCOON

The ultrastructural features of the human hair and silk cocoon membrane was studied using SEM. The results are shown in Figure 6.

ELECTRICAL CONDUCTIVITY MEASUREMENTS

Same electrode (E1:E2/Copper:Copper). The results are summarized in Figure 7.

Different electrode (E1:E2/Copper:Aluminum). The results are summarized in Figure 8.

Different electrode (E1:E2): Platinum:Aluminum.: The results are summarized in Figure 9.

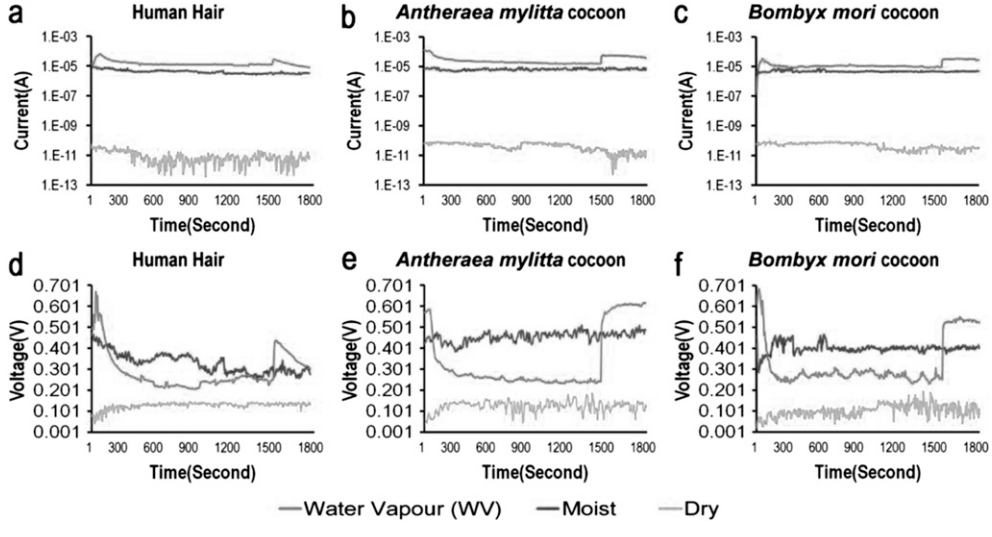

Figure 9. Electrical properties of human hair and silk cocoon sandwiched between two different electrodes namely aluminum and platinum. (A) Average (n = 6) current readings obtained using standard device for human hair under three different conditions (dry, moist, and exposed to water vapor). In dry state current is very small, as the hair is moistened current value increases then when exposed to water vapor there is further increase in the current values. (B, C) Average current recording obtained from *A. mylitta* and *B. mori* shows the same kind of pattern compared to hair. (D) Average voltage recording obtained from human hair under same conditions described earlier. The hump on the plot around 1600 s is the point where supply of water vapor was stopped. (E, F) Similar voltage readings could be seen in silk cocoon membranes.

DSC

The results are summarized in Figure 10. DSC data indicated that hydrated polymer exhibit an endothermic reaction between 50° and 80°C, which signifies rapid movement and elimination of water molecules on the polymer surface.

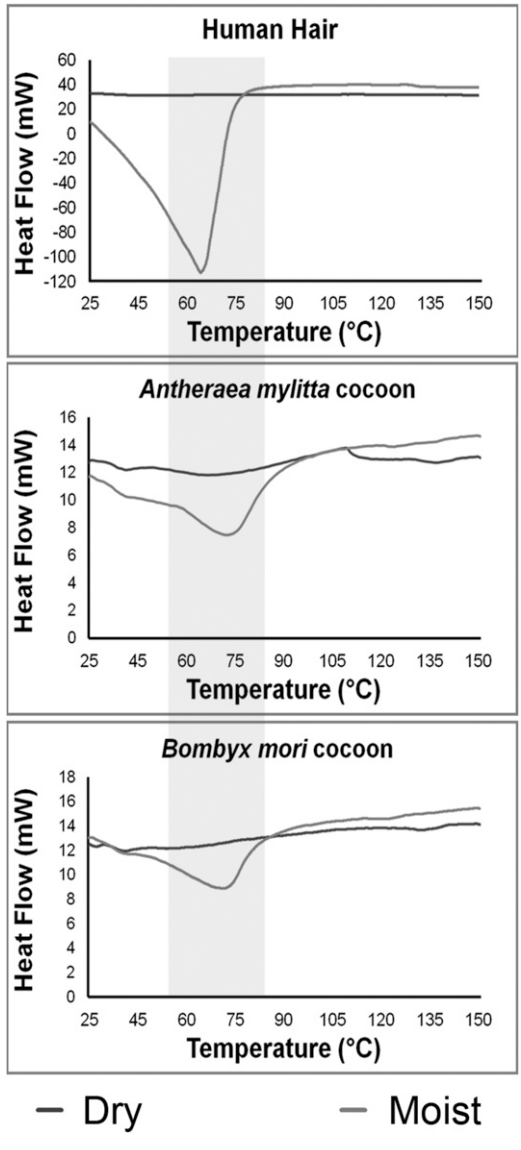

Figures 10. Shown are the DSC curves of hair and silk cocoon under two different conditions viz., without moisture and with moisture. These curves show an unique endothermic thermal event between 50° and 80°C, which resulted in rapid movement of water molecules on the surface of these polymers, thus resulting in the hopping of protons. Similar results were observed in earlier studies with keratin fibers (28–30).

DEVELOPING AN ENERGY HARVESTING BIOELECTRICAL DEVICE USING HUMAN HAIR

In order to harvest sufficient power to run a low power electronic device, we connected eight individual devices in a series circuit. Each device was prepared with aluminum and copper electrodes. The eight device series circuit assembly was mounted on a glass rod (Figure 11).

In Figure 12, we have shown the snapshots of the video showing the glowing of the video. The real-time video file is in the supplementary information.

Next, we calculated the power output of such crude devices. The power plot is shown in Figure 13.

DISCUSSION

In summary, here we showed that hair behaves like a thermo-sensitive solid polymer electrolyte. When it is exposed to "water + heat", it results in the mobilization of the inherent ionic charge carriers present in the biopolymer matrix, as well as results in the generation of large number of protons (between 50° and 80°C). By placing the hair or silk polymer between two dissimilar electrodes (with different electronegativities), we offer directionality to the ionic and proton charge carriers, thus deriving useful electricity to

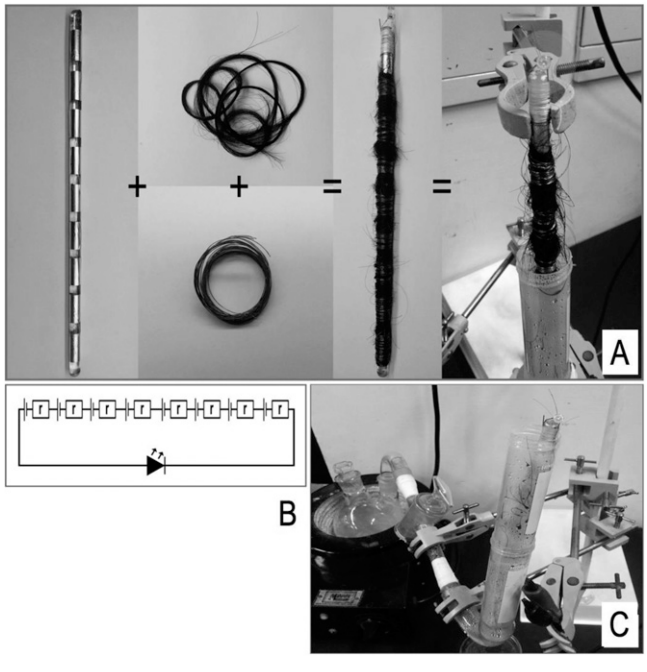

Figure 11. Hair bio-electrical device: (A) Eight devices are connected in as series circuit and the output is connected to a light-emitting diode (LED). (B) The series circuit of eight devices. (C) Glowing LED on exposure to water vapor. The LED has the following specifications. This is a very standard red LED. The lens is 3 mm in diameter, and is diffused. The features include the following: a. 1.8–2.2 VDC forward drop. b. Max current: 20 mA. c. Suggested using current: 16–18 mA. d. Luminous Intensity: 150–200 mcd.

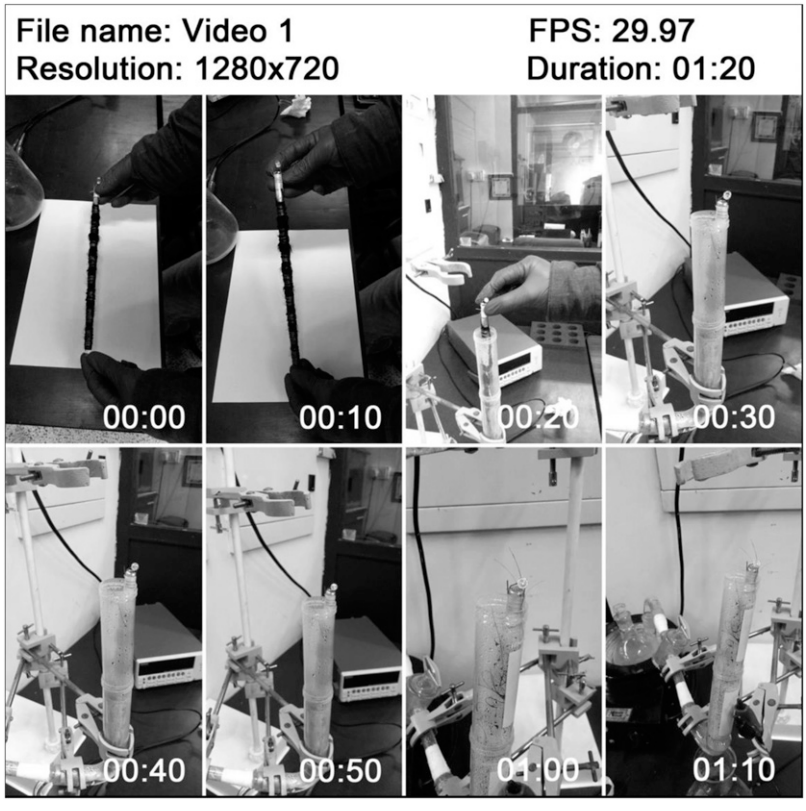

Figure 12. The snapshots of the video file showing a functional low-power electronic system deriving energy from hair bioelectric device.

run solid-state electronic devices. Thus, hair functions as a natural thermoelectric material and could be used to derive electricity from waste, moist heat.

When similar electrodes were used (Figure 7), we did not observe significant voltage or current. Further, we observed a wobbling in the voltage values. This is possibly due to the

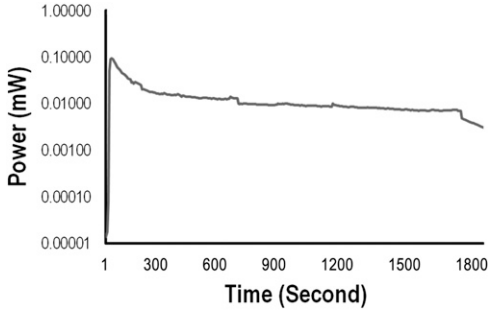

Figure 13. Power plot from "hair bioelectric device" described in Figure 9. The graph shows average (n = 6) power plot. When we exposed the hair to water vapor we get 0.01 milliwatt of power as long as the exposure to water vapor continues. As soon as the supply of water vapor was stopped the power decreased sharply. Basic electrical power equation was used to obtain the plot: Power (P) = $I\ V = R \times I^2 = V^2/R$ where power P is in watts, voltage V is in volts and current I is in amperes (DC), R is resistance in ohm. Power plot was developed using Device 2 (copper/aluminum). Since the hair polymer is fairly stable so the device exhibit significant period of longevity.

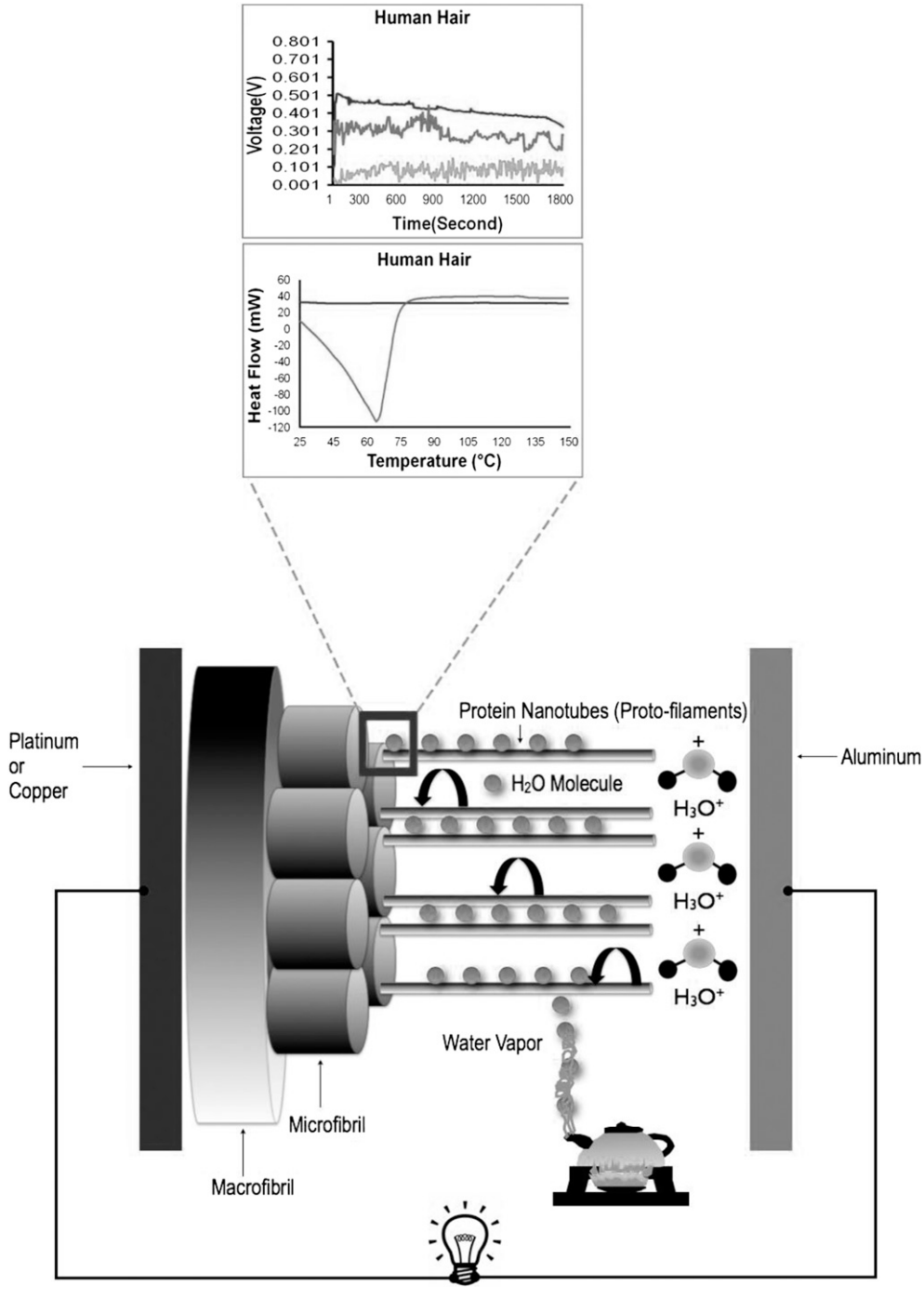

Figure 14. Proton hopping along the α-keratin tubes of hair filament, when exposed to a continuous stream of water vapor.

fact that, the similar electrodes could not offer sufficient potential difference, which would result in giving directionality to the flow of ionic charge carriers.

The fundamental question which is needed to be discussed is the generation and mobility of large number of protons on the hydrated biopolymer surface between 50° and 80°C. It was Grotthuss's study of "structural diffusion", carried out nearly two centuries ago, which offered an explanation to such anomalous high mobility of protons, in "'liquid water-polymer interface" (31–49). Subsequent refinement of this concept leads to the idea of thermal hopping (32,33), solvation effects (34), and proton tunneling (35,36).

In the light of this, we have attempted to answer the key question of this study "what is the effect of water vapor on hair that resulted in the drastic increase in its conductivity?" We speculate that apart from the inherent ions which are present in the hair, at least three other events are occurring in tandem in the presence of water vapor (Figure 14).

First, the protein filament is continuously hydrated by water vapor and water molecules occupy the vacant nano spaces of keratin tubes. These water molecules form an extensive hydrogen-bonding network along the length and breadth of the protein nanotubes.

Second, this hydrogen-bonding network is perturbed by the thermal energy contained in water vapor; forcing continuous rearrangement of the hydrogen bond network. This rearrangement generates large number of hopping protons, which almost forms a continuous proton wire along the protein nanotubes (23–26).

Third, thermal studies of keratin–water system demonstrated the rapid movement of water molecules over the hair protein surface at temperatures between 50° and 155°C (28–30). This suggests that the proton formation and proton hopping rate is further enhanced by water vapor and the continuous proton wire ensures rapid transport of protons; ensuring the flow of current (31–49). Earlier we observed similar increase in electrical conductivity in the silk–water vapor and cellulose–water vapor systems (26).

Hence, from this study, a simple bioelectric device using human hair to harness measureable electricity was developed. Although we set out to revisit a long-debated controversial question of cosmetic industry, we are penning the epilogue for a waste heat management system for thermal and nuclear power plants; where saturated water vapor is a waste byproduct. Thus, hair research, which remained confined to the cosmetics sciences, could make its way to the burgeoning arena of green and sustainable energy in future.

REFERENCES

(1) E. M. Fozard, Method and apparatus for removal of superfluous hair. Patents US2888927 A: 1959.
(2) R. F. Wagner Jr., J. M. Tornich, and D. J Grande, Electrolysis and thermolysis for permanent hair removal. *J. Am. Acad. Dermatol.,* **12,** 441–449 (1985).
(3) http://www.hairfacts.com/hair-removal-methods/doubtful-hair-removal-methods/electric-tweezers-warning/
(4) M. Feughelman, The physical properties of alpha keratin fibers. *J. Soc. Cosmet. Chem.* , **33**, 385–406 (1982).
(5) M. Feughelman, *Mechanical properties and structure of alpha-keratin fibres: wool, human hair and related fibres*. (UNSW Press, Sydney, Australia, 1997), 5, 5.
(6) J. Bradbury, The structure and chemistry of keratin fibers. *Adv. Protein Chem.,* **27,** 111–211 (1973).
(7) C. Popescu, and H. Höcker, Hair—the most sophisticated biological composite material. *Chem. Soc. Rev.,* **36,** 1282–1291 (2007).
(8) C. Popescu, and H. Höcker, Cytomechanics of hair: basics of the mechanical stability. *Int. Rev. Cell Mol. Biol.,* **277,** 137–156 (2009).

(9) J. E. McGinness, Mobility gaps: a mechanism for band gaps in melanins. *Science,* **177,** 896–897 (1972).
(10) J. McGinness, P. Corry, and P. Proctor,, Amorphous semiconductor switching in melanins. *Science,* **183,** 853–855 (1974).
(11) M. Abbas, F. D'Amico, L. Morresi, N. Pinto, M. Ficcadenti, R. Natali, L. Ottaviano, M. Passacantando, M. Cuccioloni, and M. Angeletti, Structural, electrical, electronic and optical properties of melanin films. *Eur. Phys. J. E: Soft Matter. Biol. Phys.,* **28,** 285–291 (2009).
(12) A. B. Mostert, B. J. Powell, F. L. Pratt, G. R. Hanson, T. Sarna, I. R. Gentle, and P. Meredith, Role of semiconductivity and ion transport in the electrical conduction of melanin. *Proc. Natl. Acad. Sci. USA,* **109,** 8943–8947 (2012).
(13) M. Marsh, and K. Earp, The electrical resistance of wool fibres. *Trans. Faraday Soc,* **29,** 173–192(1933).
(14) S. Baxter, Electrical conduction of textiles. *Trans. Faraday Soc.,* **39,** 207–214 (1943).
(15) J. Algie, and J. Downes, and B. Mackay, Electrical conduction in keratin. *Text. Res. J.,* **30,** 432–434 (_1960).
(16) G. King, and J. Medley, Effect of polar vapours on the direct-current conductance of keratin and nylon. *Nature,* **160,** 438-438 (1947).
(17) G. King, and J.Medley II, The influence of temperature and adsorbed salts on the DC conductivity of polar polymer adsorbate systems. *J. Colloid Sci.,* **4,** 9–18 (1949).
(18) G. King, and J. Medley, DC conduction in swollen polar polymers. I. electrolysis of the keratin-water system. *J. Colloid Sci.,* **4,** 1–7 (1949).
(19) M. Feughelman, The sorption of water by dry keratin fibers in atmospheres above 90% RH. *J. Appl. Polym. Sci.,* **2,** 189–191 (1959).
(20) M. Feughelman, A two-phase structure for keratin fibers. *Text. Res. J,* **29,** 223–228 (1959).
(21) N. E. Dorsey, Properties of ordinary water-substance. *Chem. Eng. News,* **18,** 215 (1940).
(22) N. Bjerrum, Structure and Properties of Ice, Dan. *Mat. Fys. Medd,* **27,** 1 (1951).
(23) I. Oshida, Y. Ooshika, and R. Miyasaka, Proton Transfer in Hydrogen Bond and Its Participation in π-Electron Systems. *J. Phys. Soc. Jpn,* **10,** 849–859 (1955).
(24) P. Ball, Water as an active constituent in cell biology. *Chem. Rev.*, **108,** 74–108 (2008).
(25) D. Porter, and F. Vollrath, Water mediated proton hopping empowers proteins. *Soft Matter*, **9,** 643–646 (2013).
(26) B. Tulachan, S. K. Meena, R. K. Rai, C. Mallick, T. S. Kusurkar, A.K. Teotia, N. K. Sethy, K. Bhargava, S. Bhattacharya, A Kumar, R. K Sharma, N. Sinha, S. K Singh, and M. Das Electricity from the Silk Cocoon Membrane. *Sci. Rep.*, **4,** 5434 (2014).
(27) A. O. Evans, J.M. Marsh, and R. R. Wickett, The uptake of water hardness metals by human hair. *J. Cosmet. Sci.,* **62,** 383–391(2011)
(28) R. F. Schwenker, and J. H Dusenbury, Differential thermal analysis of protein fibers. *Text. Res. J.*, **30,** 800–801 (1960).
(29) W. Humphries, D. Miller, and R. Wildnauer, The thermomechanical analysis of natural and chemically modified human hair. *J Soc Cosmet Chem.,* **23,** 359–370 (1972).
(30) P. Milczarek, M. Zielinski, and M. Garcia, The mechanism and stability of thermal transitions in hair keratin. *Colloid Polym. Sci.,* **270,** 1106–1115 (1992).
(31) C. J. T. de Grotthuss, ''Sur la de´composition de l'eau et des corps qu'elle tient en dissolution a` l'aide de l'e´lectricite´ galvanique''. *Ann. Chim.,* **58,** 54–73 (1806).
(32) E. Hückel, Theorie der Beweglichkeiten des Wasserstoff- und Hydroxylions in wässriger Lösung. *Z. Elektrochem.,* **34,** 546–562 (1928).
(33) A. E. Stearn, and Eyring, J. The deduction of reaction mechanisms from the theory of absolute rates. *J. Chem. Phys.*, **5,** 113–124 (1937).
(34) M. L. Huggins, Hydrogen bridges in ice and liquid water. *J. Phys. Chem,* **40,** 723–731 (1936).
(35) J. D. Bernal, and R. H. Fowler, R. H. Atheory of water and ionic solution, with particular reference to hydrogen and hydroxyl ions. *J. Chem. Phys.,* 1, 515–548 (1933).
(36) G. Wannier, Die Beweglichkeit des Wasserstoff- und Hydroxylions in wässeriger Lösung. *Ann. Phys., (Leipz.)* **24,** 545–590 (1935).
(37) W. Doster, The dynamical transition of proteins, concepts and misconceptions. *Eur. Biophys. J.,* **37,** 591–602 (2008).
(38) J. Guan, D. Porter, and F. Vollrath, Thermally Induced Changes in Dynamic Mechanical Properties of Native Silks. *Biomacromolecules,* **14,** 930–937 (2013).
(39) K. Tian, D. Porter, J Yao, Z Shao, and X. Chen, Kinetics of thermally-induced conformational transitions in soybean protein films. *Polymer,* S1 **11,** 2410–2416 (2010).

(40) I. Oshida, Y. Ooshika, and R. Miyasaka, Proton transfer in hydrogen bond and its participation in p-electron systems. *J. Phys. Soc. Jpn,* **10,** 849–859 (1955).
(41) E. Schauenstein, E. Treiber, W. Berndt, W. Felbinger, and H. Zima, Ultraviolett-absorptions spektren von seidenfibroin und cellulose in lithiumbromidlo¨sung. *Monatsh,* **85,** 120–139 (1954).
(42) D. Porter, and F. Vollrath, Water mediated proton hopping empowers proteins. *Soft Matter,* **9,** 643–646 (2013).
(43) P. Ball, Water as an active constituent in cell biology. *Chem. Rev.,* **108,** 74–108 (2008).
(44) D. Porter, and F. Vollrath, Water mobility, denaturation and the glass transition in proteins. *Biochim. Biophys. Acta,* **1824,** 785–791 (2012).
(45) L. Pauling, The nature of the chemical bond and the structure of molecules and crystals: an introduction to modern structural chemistry. (Cornell University Press, Ithaca, 1960), Vol 18.
(46) D. Porter, and F. Vollrath, The role of kinetics of water and amide bonding in protein stability. *Soft Matter*, **4,** 328–336 (2008).
(47) W. W. Cleland, and M. M Kreevoy, Low-barrier hydrogen bonds and enzymic catalysis. *Science*, **264,** 1887–1890 (1994).
(48) M. E. Tuckerman, D. Marx, M. L Klein, and M. Parrinello, On the quantum nature of the shared proton in hydrogen bonds. *Science,* **275,** 817–820 (1997).
(49) D. Marx, M. E Tuckerman, J. Hutter, M. Parrinello, The nature of the hydrated excess proton in water. *Nature,* **397,** 601–604 (1999).